

LP41

# Aspects corpusculaires du rayonnement. Notion de photon.

Correcteurs : Adrien Licari<sup>1</sup> et Etienne Thibierge<sup>2</sup>

Leçon présentée le jeudi 21 février 2013

## Extraits des rapports du jury

Je vous rappelle que le préambule des rapports de l'épreuve de leçon présente les attentes et exigences du jury. Je vous encourage vivement à le lire.

**2011 et 2012 :** Le transfert de quantité de mouvement est souvent présenté par le biais de l'expérience de Compton, il peut également être illustré à l'aide d'applications modernes de l'interaction atome-rayonnement. Cette leçon peut éventuellement permettre de parler de la notion de superposition d'états. Au cours des questions, le jury a été surpris de constater que la notion de spin associée à un photon n'est pas toujours maîtrisée. Le jury invite les candidats à réfléchir sur la physique à l'oeuvre à l'échelle de la longueur d'onde Compton.

**2009 et 2010 :** Les expériences réalisées à l'aide d'une cellule photoélectrique sont souvent mal comprises ou interprétées abusivement. Les candidats cernent souvent mal pourquoi la notion de photon s'est dégagée de l'effet photoélectrique et du corps noir.

**Changement de titre :** jusqu'en 2007, la leçon s'intitulait *Le photon : la particule et ses interactions avec la matière*.

**2007 :** Cette partie importante de la physique quantique est mal couverte par les manuels usuels. Le photon a une énergie, une quantité de mouvement, mais aussi un moment cinétique. Les illustrations ne se limitent pas à l'effet photo-électrique et à l'effet Compton, et les récents développements de la physique quantique constituent une mine d'illustrations pour cette leçon : ralentissement d'atomes par la lumière, interférences avec des photons uniques, comportement de la lumière sur une lame semi-réfléchissante ...

**2004 :** Des expériences doivent être décrites et modélisées en donnant des ordres de grandeur. Les échanges de moment cinétique méritent d'être discutés.

## Commentaires généraux

La leçon présentée était trop longue et a dû être interrompue au début de la partie 3.2.

Le contenu est globalement correct et maîtrisé, sans erreur de fond, et rien n'est hors sujet. On peut toutefois discuter la pertinence de certains choix pour une leçon d'agrégation.

Cependant, la présentation était confuse. Elle ressemblait trop souvent à une suite de calculs alors que les raisonnements physiques et les hypothèses n'étaient pas assez mis en avant. La démarche suivie dans la leçon n'est pas suffisamment apparente : on doit savoir à tout moment d'où vous partez et où vous souhaitez aller. C'est d'autant plus important dans cette leçon qu'il n'est pas possible d'y démontrer les résultats sur le photon de façon rigoureuse, puisque cela nécessiterait l'électrodynamique quantique. Les choix et les partis pris doivent donc être explicités avec un soin particulier, en particulier lors des raisonnements utilisant l'électromagnétisme classique.

Une leçon doit s'inscrire dans un cadre pédagogique vraisemblable, qui se traduit par les prérequis et un niveau académique à annoncer en début de leçon. Vous ne pouvez pas supposer raisonnablement que des étudiants n'ont jamais entendu parler de photon alors qu'ils connaissent la physique statistique, la biréfringence, la théorie des bandes et la mer de Fermi ! Au delà des prérequis, le rapport à la mécanique quantique dans la leçon présentée pose question. Le choix de discuter en si peu de temps la cryptographie quantique est à cet égard très discutable.

Parmi tous les ouvrages cités en bibliographie, celui de B. Cagnac est particulièrement intéressant pour cette leçon. L'édition la plus récente est largement complétée par rapport aux précédentes.

## Retour sur la leçon présentée

### Introduction

L'introduction doit poser le problème de la leçon, et le relier aux prérequis. C'est aussi l'occasion d'annoncer clairement la démarche qui sera suivie dans la leçon, sans en faire une annonce de plan guindée. C'est particulièrement important dans cette leçon, et ça a un peu manqué.

### 1) Nature corpusculaire du rayonnement

#### 1/ Corps noir

La présentation suivie était complète et rapide. Le corps noir faisant l'objet d'une leçon, il est tout à fait justifié de le placer en prérequis, et de se contenter de rappeler les résultats majeurs sans les démontrer.

La catastrophe UV de la théorie de Rayleigh-Jeans ne concerne pas vraiment le fait que  $\int_0^\infty u(\nu, T) d\nu$  diverge, mais plutôt la divergence de  $u(\nu, T)$  lorsque  $\nu \rightarrow \infty$ , même si la deuxième divergence entraîne évidemment la première.

1. adrien.licari@ens-lyon.fr

2. etienne.thibierge@ens-lyon.fr, <http://perso.ens-lyon.fr/etienne.thibierge>

## 2/ Effet photoélectrique

Les expériences de leçon doivent être présentées avec méthode : commencez par projeter un schéma, puis présentez les éléments du montage en lien avec le schéma, et enfin réalisez l'expérience. Commencer par réaliser l'expérience avant de la présenter ne permet pas à l'auditoire de bien suivre ce qui se passe.

Il ne faut pas se précipiter en réalisant l'expérience : le mouvement de l'aiguille de l'électroscope est parfois assez lent. En outre, il arrive qu'au lieu de charger l'électroscope en électrons on lui en arrache, empêchant l'effet de se manifester. Testez donc bien l'expérience avant de la présenter au jury !

C'est une bonne idée d'avoir projeté des courbes expérimentales tirées de la banque d'images, mais attention à ne pas se faire piéger : il faut savoir répondre aux questions les concernant, et c'était le cas ici.

Parler d'énergie de Fermi lors de l'exposé est d'un niveau trop avancé (c'est en revanche parfait pour les questions). Il faut se restreindre au travail de sortie, qu'on considérera comme une grandeur phénoménologique.

L'effet photoélectrique étant très classique, il faut le présenter impeccablement. Cagnac en donne une discussion très claire.

## II) Caractéristiques du photon et interactions avec la matière

Cette partie est délicate à présenter, car y faire des démonstrations rigoureuses est impossible. Au mieux, on y établit des conditions pour que la notion de photon ne soit pas contradictoire avec l'électromagnétisme et la relativité. Il faut donc être extrêmement clair sur ce qu'on suppose et ce qu'on déduit.

### 1/ Effet Compton

Le raisonnement utilisé pour trouver la masse du photon ne me convainc pas vraiment, pour ne pas dire vraiment pas. Parler de la relation entre  $E$  et  $\vec{p}$  comme la relation de dispersion est exact en mécanique quantique ... mais déplacé dans cette leçon, où la dualité onde-corpuscule n'est pas encore introduite en entier.

Lorsque l'on écrit les composantes des quadri-vecteurs, il est indispensable de préciser le référentiel dans lequel on se place.

Le calcul détaillé de l'effet Compton est assez lourd et fastidieux. Il n'est pas absurde de le faire dans cette leçon, néanmoins je ne suis pas sûr que ce soit le meilleur choix. Je pense qu'on pourrait se contenter de présenter les résultats expérimentaux, la physique du problème, d'écrire les quadri-vecteurs avant et après la collision, et de dire « le calcul donne ».

### 2/ Effet de recul

### 3/ Création de paires

Ces deux parties sont intéressantes dans l'absolu, mais leur présentation les rend peu digestes.

Elles donnent aussi l'impression d'un effet catalogue : on ne voit pas bien ce qu'elles apportent de plus que l'effet Compton à la compréhension de la notion de photon.

Présenter trois expériences utilisant la conservation du quadri-vecteur ( $E/c, \vec{p}$ ) me semble excessif au vu des possibilités de la leçon.

## 4/ Transfert de moment cinétique

L'utilisation d'un modèle purement classique ne peut pas se faire sans précaution dans le discours. Je trouve la démarche choisie pertinente, mais il faut vraiment expliquer les objectifs du calcul et ce que l'on suppose acquis.

Attention aux lapsus dans le discours : le moment cinétique d'une force n'existe pas !

L'expérience de Beth est pertinente et intéressante, mais ne peut pas être présentée qu'à l'oral. Comme à chaque fois que vous présentez une expérience, **il faut** projeter un schéma du dispositif, sous peine de perdre votre auditoire.

## III) Applications actuelles

Ce choix de dernière partie me semble pertinent, et une multitude d'expériences peuvent être présentées. Vous devez les choisir avec soin, leur interprétation ne devant pas faire appel à des notions de mécanique quantique trop avancées.

### 1/ Refroidissement d'atomes

La pression de radiation en EM classique peut être supposée connue, mais si vous faites ce choix il faut le préciser dans les prérequis.

La présentation choisie, inspirée de Dangoisse, est satisfaisante. Elle permet de faire sentir simplement toute la physique du phénomène.

### 2/ Cryptographie quantique

La présentation de cette partie n'a pas pu être menée à son terme par manque de temps.

Je pense que la cryptographie est beaucoup trop compliquée pour être présentée brièvement en fin de leçon. La notion de superposition d'états et la notion d'état propre de l'appareil de mesure doivent être présentées avec douceur (il me semble délicat de les mettre en prérequis). Par conséquent, le temps nécessaire est assez long, et peut difficilement être réduit.

Le choix de tout faire sur transparent n'est pas optimal. De plus, il est inutile d'y écrire du texte que l'auditoire n'a pas le temps de lire.

## Questions

Les questions servent *d'abord* à éclaircir les points peu clairs de la leçon, puis *ensuite* à tester vos connaissances plus largement. Voilà quelques notions sur des points qui pourraient être discutés lors des questions.

Un photomultiplicateur exploite directement l'effet photoélectrique. Duffait et Sextant décrivent bien son fonctionnement.

Les relations  $E = h\nu$  et  $E = hc/\lambda$  n'ont pas du tout le même statut. La première est une des relations de de Broglie, et fait partie des postulats de la mécanique quantique. Elle s'applique donc à n'importe quelle particule.

La seconde s'en déduit en utilisant la relation de dispersion du photon dans le vide  $\nu = c/\lambda$ , et n'est donc vraie que dans ce cas précis.

En tant que particule quantique relativiste, un photon n'obéit pas à l'équation de Schrödinger, mais à l'équation de Klein-Gordon. Pour une particule de masse nulle, celle-ci se réduit à l'équation de d'Alembert.

On entend parfois que le corps noir et l'effet photoélectriques constituent des preuves expérimentales de l'existence du photon, ce qui est en fait faux. Ces deux effets pourraient s'expliquer à l'aide d'un modèle considérant le champ EM classique et la matière avec niveaux d'énergie quantifiés. Une vraie preuve expérimentale a été apportée par Philippe Grangier, Gérard Roger et Alain Aspect en 1986. L'idée de l'expérience est très simple : il s'agit d'envoyer de la lumière sur une lame semi-réfléchissante, et de mesurer les corrélations entre lumière réfléchie et lumière transmise. Je joins à ce corrigé l'article original, ainsi qu'un autre article de Thorn *et al.* qui explique la théorie de façon plus simple.

L'effet photoélectrique et l'effet Compton mettent tous les deux en jeu une collision électron-photon, mais donnent lieu à une physique nettement différente. La collision Compton est une collision *élastique*, où l'on peut écrire la conservation du quadrivecteur énergie-impulsion. Au contraire, la collision photoélectrique est *inélastique* : le photon incident est détruit et son énergie n'est pas entièrement convertie en énergie cinétique de l'électron, puisqu'une partie constitue le travail d'extraction.

La notion de spin du photon est un peu subtile. La direction de quantification canonique est la direction de propagation, on parle alors d'*héllicité* du photon. Le photon est un boson de spin 1 (en unités de  $\hbar$ ), dont le spin pourrait alors *a priori* prendre les valeurs  $-1, 0$  ou  $1$ , **mais** la valeur  $0$  est interdite. Il n'y a pas d'explication simple à donner, la raison profonde est une incompatibilité entre spin  $0$  et masse nulle en électrodynamique quantique.

Un peu de culture sur le refroidissement d'atomes et les condensats de Bose-Einstein, merci Charlotte! Voilà une "recette" pour faire des condensats :

- ▷ On ralentit d'abord un jet d'atomes avec un laser à résonance allant en sens opposé au jet. Pour compenser l'effet Doppler et le changement de fréquence apparente au cours du ralentissement, on utilise un ralentisseur à effet Zeeman qui crée un gradient de champ magnétique tout le long du ralentissement.
- ▷ Une fois qu'ils sont à une vitesse faible (20 cm/s), on les piège en allumant six faisceaux contra-propageants dans les trois directions de l'espace. On obtient une mélasse optique. La force qui retient les atomes est une force de frottement visqueux (pression de radiation). C'est le principe du refroidissement Doppler présenté par Timothée dans une direction de l'espace. Avec une mélasse optique, on ne piège pas les atomes durablement. Il faut un piège magnéto-optique : on rajoute un gradient de champ magnétique qui correspond à l'analogie d'une force de rappel pour les atomes vers le centre du piège. Dans un piège magnéto-optique la température est de  $100 \mu\text{K}$ .
- ▷ Pour arriver au condensat, il faut réaliser un refroidissement par évaporation consistant à diminuer la pro-

fondeur d'un piège (optique ou magnétique) : on perd des atomes mais on garde les plus froids donc dans l'ensemble, on refroidit. Et là on peut arriver aux températures de condensation, environ 100 nK.

## Une approche possible

Voici une proposition de construction de la leçon. Le plan resterait voisin de celui qui a été présenté, mais en insistant beaucoup plus sur la démarche pédagogique. **Il ne s'agit que d'une proposition, qui n'engage que moi! Il y a bien sûr d'autres façons de procéder.**

### I) Caractère corpusculaire du rayonnement

La première partie a pour but de présenter l'intérêt de la notion de photon et la façon dont elle a émergé historiquement. On présente donc les principaux résultats sur le rayonnement du corps noir et l'intérêt de l'hypothèse de Planck, sans s'apesantir puisque le corps noir fait partie des prérequis.

On s'intéresse ensuite à l'effet photoélectrique, que l'on montre expérimentalement. On en fait une discussion complète [Cagnac], en insistant sur l'apport de la notion de photon à l'interprétation. En conclusion de cette partie, on postule qu'une onde électromagnétique se décrit comme un paquet de particules appelées photons, chaque photon transportant une énergie  $E = h\nu$ .

### II) Caractéristiques d'un photon

Une fois formulé ce postulat, la deuxième partie s'attache à obtenir les caractéristiques cinétiques du photon (masse, quantité de mouvement, moment cinétique). Le raisonnement suivi consiste à dire que la description en termes de photon ne doit pas être contradictoire avec ce que l'on sait de l'électromagnétisme et de la relativité. On réinterprète donc des résultats d'EM classique en termes de photons, et on en déduit des conditions pour que l'ensemble ne soit pas incohérent.

On commence par la pression de radiation, pour arriver à  $\vec{p} = \hbar\vec{k}$ . On s'intéresse ensuite à la masse du photon. En utilisant la relation d'Einstein de la relativité, on en déduit qu'il faut qu'elle soit nulle pour qu'il n'y ait pas de contradiction. Enfin, on parle du moment cinétique du photon à partir du moment exercé sur une lame quart d'onde [Cagnac].

On peut aussi obtenir ces résultats à partir d'un modèle simple d'atome, extrait du sujet d'agrégation 2001, et présenté dans les exercices corrigés du Dunod de spé, ch. OEM dans le vide.

### III) Expériences à photons

La troisième partie consiste à illustrer ces notions en présentant des expériences. Elle est très ouverte, et son contenu dépend de votre sensibilité et de votre « culture photonique ». Pensez à lui réserver suffisamment de temps, car le jury s'attend à voir autre chose que seulement des calculs d'électromagnétisme classique.

Pour ma part, je présenterais l'effet Compton qui est très classique et qui est réutilisable dans la LP dynamique

relativiste [Cagnac], et l'expérience de Grangier *et al.* [articles joints]. Mais de nombreux autres choix sont possibles, et on peut tout à fait parler de l'expérience de Beth, du refroidissement d'atomes, d'interférences d'un photon avec lui-même, . . . Le tout est que vos choix soient cohérents avec le cadre pédagogique de la leçon, et que vous soyez capables de répondre à quelques questions dessus.

Pour utiliser des articles le jour de l'oral, il faut envoyer les revues contenant ces articles. La bibliothèque possède aussi bien *Europhysics Letters* que *American Journal of Physics* en collection papier.

## Conclusion

La leçon présentée contient un certain nombre de bonnes idées, mais la démarche suivie est trop floue et ne les met donc pas en valeur. Soyez particulièrement vigilants sur ce point lorsque vous préparerez votre propre leçon.

Si vous avez d'autres questions, nous restons à votre disposition par mail, en TP ou dans de futures séances de correction.

EUROPHYSICS LETTERS

15 February 1986

*Europhys. Lett.*, **1** (4), pp. 173-179 (1986)

## Experimental Evidence for a Photon Anticorrelation Effect on a Beam Splitter: A New Light on Single-Photon Interferences.

P. GRANGIER, G. ROGER and A. ASPECT (\*)

*Institut d'Optique Théorique et Appliquée, B.P. 43 - F 91406 Orsay, France*

(received 11 November 1985; accepted in final form 20 December 1985)

PACS. 42.10. – Propagation and transmission in homogeneous media.

PACS. 42.50. – Quantum optics.

**Abstract.** – We report on two experiments using an atomic cascade as a light source, and a triggered detection scheme for the second photon of the cascade. The first experiment shows a strong anticorrelation between the triggered detections on both sides of a beam splitter. This result is in contradiction with any classical wave model of light, but in agreement with a quantum description involving single-photon states. The same source and detection scheme were used in a second experiment, where we have observed interferences with a visibility over 98%.

During the past fifteen years, nonclassical effects in the statistical properties of light have been extensively studied from a theoretical point of view [1], and some have been experimentally demonstrated [2-7]. All are related to second-order coherence properties, via measurements of intensity correlation functions or of statistical moments. However, there has still been no test of the conceptually very simple situation dealing with single-photon states of the light impinging on a beam splitter. In this case, quantum mechanics predicts a perfect anticorrelation for photodetections on both sides of the beam splitter (a single-photon can only be detected once!), while any description involving classical fields would predict some amount of coincidences. In the first part of this letter, we report on an experiment close to this ideal situation, since we have found a coincidence rate, on both sides of a beam splitter, five times smaller than the classical lower limit.

When it comes to single-photon states of light, it is tempting to revisit the famous historical «single-photon interference experiments» [8]. One then finds that, in spite of their

---

(\*) Also with Collège de France, Laboratoire de Spectroscopie Hertzienne de l'ENS, 24 rue Lhomond, 75005 Paris 5ème.

denomination <sup>(1)</sup>, none has been performed with single-photon states of light. As a matter of fact, all have been carried out with chaotic light, for which it is well known that quantum second-order coherence properties cannot be distinguished from classical ones, even with a strongly attenuated beam [9]. This is why we have carried out an interference experiment with the same apparatus as used in the first experiment, *i.e.* with light for which we have demonstrated a property characteristic of single-photon states. This single-photon interference experiment is described in the second part of this letter.

Our experimental scheme uses a two-photon radiative cascade described elsewhere [10], that emits pairs of photons with different frequencies  $\nu_1$  and  $\nu_2$ . The time intervals between the detections of  $\nu_1$  and  $\nu_2$  are distributed according to an exponential law, corresponding to the decay of the intermediate state of the cascade with a lifetime  $\tau_s = 4.7$  ns.

In the present experiment (fig. 1), the detection of  $\nu_1$  acts as a trigger for a gate generator, enabling two photomultipliers in view of  $\nu_2$  for a duration  $w \approx 2\tau_s$ . These two photomultipliers, on both sides of the beam splitter BS, feed singles' and coincidences' counters. We denote  $N_1$  the rate of gates,  $N_t$  and  $N_r$  the singles' rates for  $PM_t$  and  $PM_r$ , and  $N_c$  the coincidences' rate. Our measurements yield the probabilities for singles' counts during  $w$ :

$$p_t = \frac{N_t}{N_1}, \quad p_r = \frac{N_r}{N_1}, \quad (1a)$$

and the probability for a coincidence

$$p_c = \frac{N_c}{N_1}. \quad (1b)$$

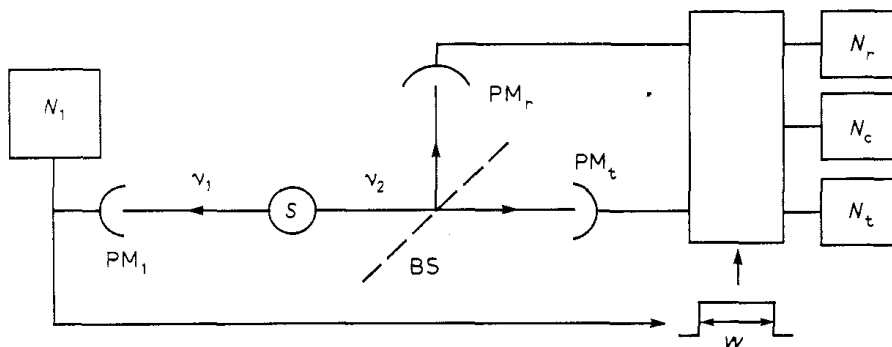


Fig. 1. – Triggered experiment. The detection of the first photon of the cascade produces a gate  $w$ , during which the photomultipliers  $PM_t$  and  $PM_r$  are active. The probabilities of detection during the gate are  $p_t = N_t/N_1$ ,  $p_r = N_r/N_1$  for singles, and  $p_c = N_c/N_1$  for coincidences.

<sup>(1)</sup> Usually, the single-photon character is stated by showing that the amount of energy flowing during a certain characteristic time (coherence time, or time of flight between source and detector) is small compared to  $h\nu$ . The necessity of the concept of photon is thus postulated, probably on the basis that the detection process appears discrete. But it is well known that this argument is not fully conclusive, since all the characteristics of the photoelectric effect can be assigned to the fact that the «atomic detector is controlled by the laws of quantum mechanics» (see ref. [1], or: W. E. LAMB and M. O. SCULLY, in *Polarisation, Matière et Rayonnement*, ed. Société Française de Physique, Presses Universitaires de France, 1969).

During a gate, the probability for the detection of a photon  $\nu_2$ , coming from the same atom that emitted  $\nu_1$ , is much bigger than the probability of detecting a photon  $\nu_2$  emitted by any other atom in the source. We are then in a situation close to an ideal single-photon state emission, and we can expect the characteristic behaviour of such a state, *i.e.* an anticorrelation between detections occurring on both sides of the beam splitter.

We calculate now the minimum coincidence rate predicted by a classical wave-description of the experiment of fig. 1, involving the intensity  $I(t)$  impinging on the beam splitter. Let us define the time-averaged intensity for the  $n$ -th gate, open at time  $t_n$ :

$$i_n = \frac{1}{w} \int_{t_n}^{t_n+w} I(t) dt . \quad (2)$$

The semi-classical model of photodetection (see footnote <sup>(1)</sup>) yields

$$p_t = \alpha_t w \langle i_n \rangle , \quad p_r = \alpha_r w \langle i_n \rangle , \quad (3a)$$

$$p_c = \alpha_t \alpha_r w^2 \langle i_n^2 \rangle , \quad (3b)$$

where  $\alpha_t$ ,  $\alpha_r$  are global detection efficiencies, and brackets indicate averages defined over the ensemble of gates:

$$\langle i_n \rangle = \frac{1}{N_1 T} \sum_{n=1}^{N_1 T} i_n , \quad (4a)$$

$$\langle i_n^2 \rangle = \frac{1}{N_1 T} \sum_{n=1}^{N_1 T} i_n^2 \quad (4b)$$

( $T$  is the total duration of the experiment).

The standard Cauchy-Schwarz inequality:

$$\langle i_n^2 \rangle \geq \langle i_n \rangle^2 \quad (5)$$

holds for our average. Therefore, a classical description of this «triggered experiment» would yield counting rates obeying the inequality

$$p_c \geq p_r p_t , \quad (6)$$

or equivalently

$$\alpha \geq 1 \quad \text{with} \quad \alpha = \frac{p_c}{p_r p_t} = \frac{N_c N_1}{N_r N_t} . \quad (7)$$

These inequalities mean clearly that the classical coincidence probability  $p_c$  is always greater than the «accidental coincidence» probability, which is equal to  $p_r p_t$ . The violation of inequality (7) thus gives an «anticorrelation» criterion, for characterizing a nonclassical behaviour.

The actual values of the counting rates for our experiment are obtained by a straightforward quantum-mechanical calculation. Denoting  $N$  the rate of excitation of the cascade, and  $\varepsilon_1$ ,  $\varepsilon_t$  and  $\varepsilon_r$  the detection efficiencies (including collection solide angle, optics

transmission, and detector efficiency), we obtain

$$N_1 = \varepsilon_1 N , \quad (7a)$$

$$N_t = N_1 \varepsilon_t (f(w) + Nw) , \quad (7b)$$

$$N_r = N_1 \varepsilon_r (f(w) + Nw) , \quad (7b')$$

$$N_c = N_1 \varepsilon_t \varepsilon_r (2f(w)Nw + (Nw)^2) . \quad (7c)$$

The quantity  $f(w)$ , very close to 1 in our experiment, is the product of the factor  $1 - \exp[-w/\tau_s]$  (overlap between the gate and the exponential decay in the cascade) by a factor slightly greater than one related to the angular correlation between  $\nu_1$  and  $\nu_2$  [11].

The comparison of eqs. (7b), (7b') and (7c) clearly shows the anticorrelation: there is a «missing term»  $(f(w))^2$  in  $N_c$ , related to the fact that a single photon can only be detected once. The quantum-mechanical prediction for  $\alpha$  is thus

$$\alpha_{\text{QM}} = \frac{2f(w)Nw + (Nw)^2}{(f(w) + Nw)^2} , \quad (8)$$

which is smaller than one. The corresponding effect will be strong if  $Nw$  can be chosen much smaller than  $f(w)$ ; the experiment is thus designed in order to satisfy this requirement.

The excitation of the atoms is achieved by a two-photon process, using two single-line laser at different frequencies [10]. Several feedback loops control the laser frequencies and intensities, in order to obtain a short- and long-term stability of the excitation rate  $N$  within a few percent. The gate  $w$  is realized using two time-to-amplitude converters followed by threshold circuits. These «single-channel analysers» are fed by shaped pulses from  $\text{PM}_1$  on the START input, and from  $\text{PM}_t$  or  $\text{PM}_r$  on the STOP input. The gates corresponding to  $N_t$  and  $N_r$  can thus be adjusted and superimposed within 0.1 ns. A third time-to-amplitude converter measures the elapsed times between the various detections, and allows a permanent control of the gating system.

The value of  $w$  is chosen for a maximum violation of the semi-classical inequality  $\alpha \geq 1$ , by maximizing the quantity  $(1 - \alpha)/\sigma_\alpha$ , where  $\sigma_\alpha$  is the standard deviation on the measurement of  $\alpha$  due to the counting process. This criterion yields  $w = 9$  ns.

In fig. 2 the theoretical and experimental values of  $\alpha$  are plotted as a function of  $Nw$  (see

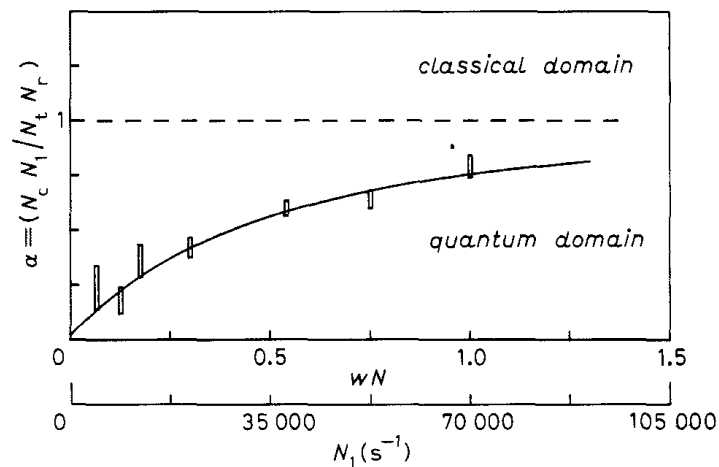


Fig. 2. – Anticorrelation parameter  $\alpha$  as a function of  $wN$  (number of cascades emitted during the gate) and of  $N_1$  (trigger rate). The indicated error bars are  $\pm$  one standard deviation. The full-line curve is the theoretical prediction from eq. (8). The inequality  $\alpha \geq 1$  characterizes the classical domain.

eq. (8)), or equivalently as a function of the rate of gates  $N_1 = \varepsilon_1 N$ . A maximum violation of more than 13 standard deviations is obtained for  $\alpha = 0.18 \pm 0.06$ . For this point, the total counting time was  $T \approx 5$  hours, with  $N_1 \approx 8800 \text{ s}^{-1}$  (including the dark rate  $300 \text{ s}^{-1}$ ), and  $N_r \approx 5 \text{ s}^{-1}$  (dark rate  $0.02 \text{ s}^{-1}$ ). In that case, the number of expected coincidences from the classical theory would be  $N_c^{\text{class}} T \geq 50$ , while we found  $N_c^{\text{exp}} T = 9$ . Hence the light emitted after each «triggering» pulse has been shown to exhibit a specifically quantum anti-correlation behaviour <sup>(2)</sup>.

By building a Mach-Zehnder interferometer around the beam splitter BS1 (fig. 3), an actual «single-photon» interference experiment can be designed. According to quantum mechanics, the probabilities  $p_{\text{MZ1}}$  and  $p_{\text{MZ2}}$  for a detection during the gate in either output of the interferometer are oppositely modulated, as a function of the path difference  $\delta$ , with a visibility unity.

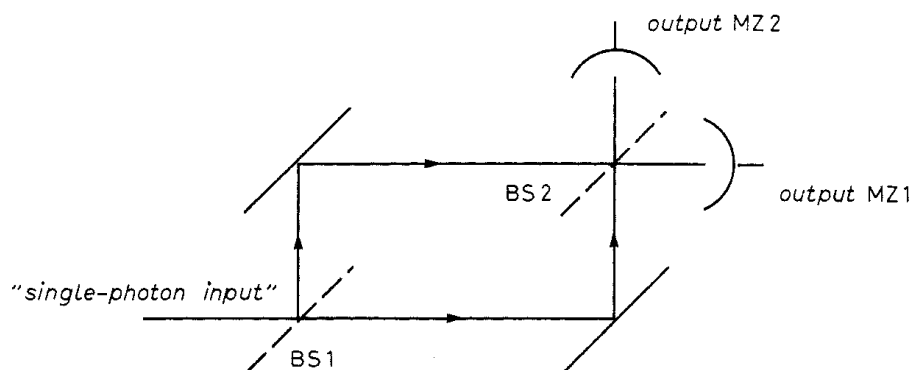


Fig. 3. – Mach-Zehnder interferometer. The detection probabilities in outputs MZ1 and MZ2 are oppositely modulated as a function of the path difference between the arms of the interferometer.

In the actual experiment, the optical system is designed in order to accept the large optical spread of the beam from the source [10] (beam diameter 40 mm for a total divergence 25 mrd), without destroying the visibility of the fringes. This was achieved by observing the fringes in the focal planes of two lenses in view of the outputs MZ1 and MZ2, and working at a path difference around zero.

The two beam splitters BS1 and BS2 are actually two multielectric coatings on a single ( $60 \times 120$ ) mm<sup>2</sup> silica plate. The planeities of this plate and of the mirrors are close to  $\lambda/50$ ; the orientations are controlled by mechanical stages at about the same precision. The counting rates on both outputs of the interferometer are measured as a function of the path difference  $\delta$ ;  $\delta$  is varied using a piezo-driven mechanical system, which ensures a parallel translation of the mirror at the required precision.

The interferometer was first checked using light from the actual source, but without any gating system. We found a fringe visibility <sup>(3)</sup>  $V = 98.7\% \pm 0.5\%$ , easily reproducible from

<sup>(2)</sup> A counter experiment has been performed using a pulsed photodiode; the rate  $N_1$  of exciting electrical pulses, and the probabilities  $p_t = N_t/N_1$  and  $p_r = N_r/N_1$  can be adjusted to the same values than in the actual experiment. But since the light pulse from the diode can be described classically, the expected number of coincidences obeys inequality (7). This point has been verified experimentally in detail.

<sup>(3)</sup> The fringe visibility is defined by  $V = (N_{\text{MZ1}}^{\text{Max}} - N_{\text{MZ1}}^{\text{Min}})/(N_{\text{MZ1}}^{\text{Max}} + N_{\text{MZ1}}^{\text{Min}})$ , where  $N_{\text{MZ1}}^{\text{Max}}$  and  $N_{\text{MZ1}}^{\text{Min}}$  are the maximum and minimum counting rates on output MZ1 when  $\delta$  is varied (dark rates of the PMTs are subtracted for this calculation).

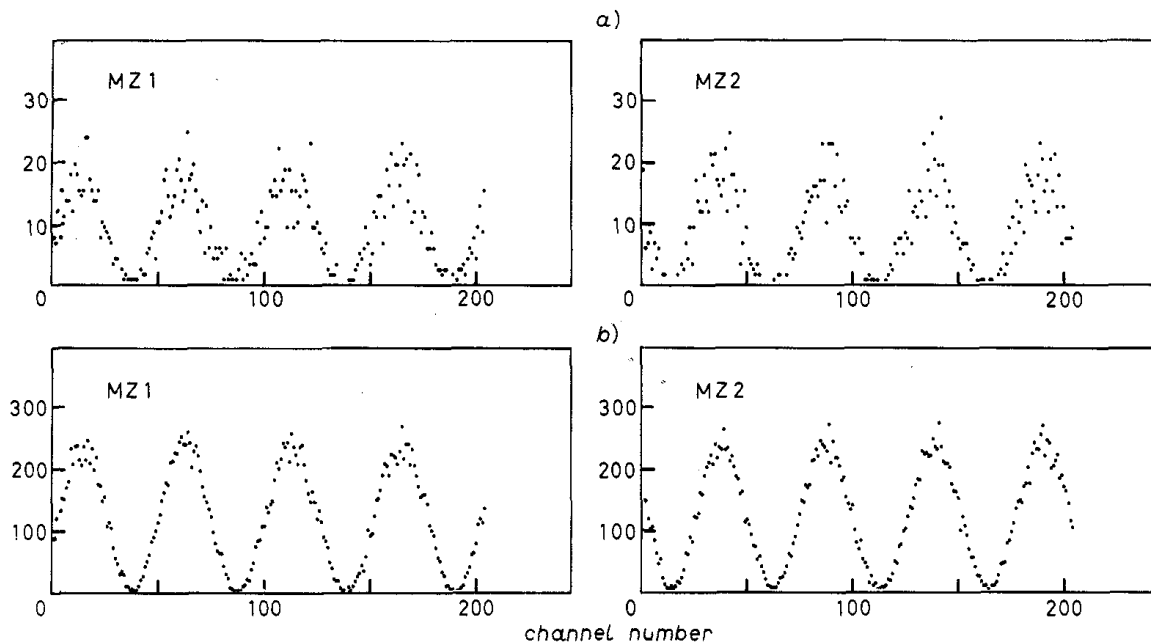


Fig. 4. - Number of counts in outputs MZ1 and MZ2 as a function of the path difference  $\delta$  (one channel corresponds to a  $\lambda/50$  variation of  $\delta$ ). a) 1 s counting time per channel b) 15 s counting time per channel (compilation of 15 elementary sweeps (like (a))). This experiment corresponds to an anticorrelation parameter  $\alpha = 0.18$ .

day to day within the error limit. In the actual gated experiment,  $\delta$  was varied around  $\delta = 0$  over 256 steps of  $\lambda/50$  each, with a counting time of 1 s per step. These sweeps over 5 fringes were stored separately into a computer, then compiled to improve the signal-to-noise ratio. A single sweep and the compiled result for  $\alpha = 0.18$  are shown on fig. 4. Several methods of data analysis consistently yielded  $V > 98\%$  for any value of  $\alpha$  (fig. 5).

Two triggered experiments have thus been performed, using the same source and the same triggering scheme for the detectors. They illustrate the wave-particle duality of light. Indeed, if we want to use classical concepts, or pictures, to interpret these experiments, we must use a particle picture for the first one («the photons are not split on a beam splitter»), since we violate an inequality holding for any classical wave model. On the contrary, we are compelled to use a wave picture («the electromagnetic field is coherently

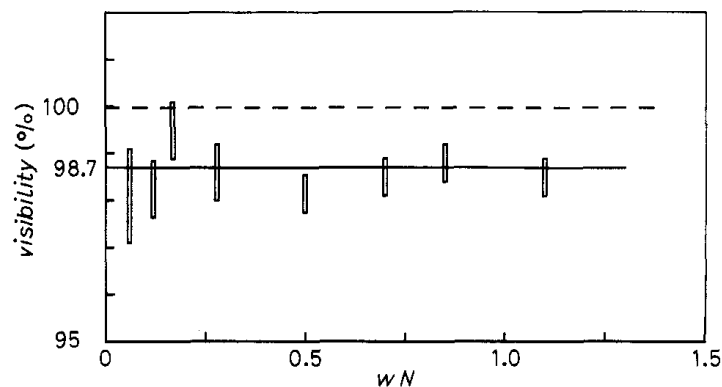


Fig. 5. - Visibility of the fringes in the single-photon regime as a function of  $wN$  (compare with fig. 2). A correction (smaller than 0.3%) has been made for dark counts of the PMTs. The estimation of the error bars is conservative.

split on a beam splitter») to interpret the second (interference) experiment. Of course, the two complementary descriptions correspond to mutually exclusive experimental set-ups <sup>(4)</sup>.

From the point of view of quantum optics, we will rather emphasize that we have demonstrated a situation with some properties of a «single-photon state». An ideal source of such states would involve the collection of the light at frequency  $\nu_2$  in a  $4\pi$  solid angle, and a shutter triggered by the photons  $\nu_1$ . One could then carry out many experiments related to nonclassical properties of light, for instance production of sub-Poisson light [12] <sup>(5)</sup>.

Although such a scheme can be considered, it would be extremely hard to work out, for practical reasons. Nevertheless, there exists a similar scheme that seems more promising: it consists of pairs of photons emitted in parametric splitting [2, 13, 14]. Due to the phase matching condition, the angular correlation between photons  $\nu_1$  and  $\nu_2$  is very strong and it becomes possible to produce single-photon states in a single spatial mode.

\* \* \*

The authors acknowledge support from Direction des Recherches, Etudes et Techniques, grant No. 81/215.

---

<sup>(4)</sup> The discussion (and possibly the experiment) can be refined by considering a «quantum nondemolition measurement» of the passage of photons in one arm of the interferometer (N. IMOTO, H. A. HAUS and Y. YAMAMOTO: *Phys. Rev. A*, **32**, 2287 (1985) and references therein). Such a device would entail phase fluctuations destroying the interference pattern.

<sup>(5)</sup> Instead of the «deletion» scheme proposed in [12], one could also use a feedback loop, activated by  $\nu_1$ , and reacting on the cascade rate, in order to quiet the Poisson fluctuations in the number of cascades excited in a certain time. See also ref. [14].

## REFERENCES

- [1] For a review, see: R. LOUDON: *Rep. Prog. Phys.*, **43**, 913 (1980).
- [2] D. C. BURNHAM and D. L. WEINBERG: *Phys. Rev. Lett.*, **25**, 84 (1970); S. FRIBERG, C. K. HONG and L. MANDEL: *Phys. Rev. Lett.*, **54**, 2011 (1985).
- [3] J. F. CLAUSER: *Phys. Rev. D*, **9**, 853 (1974).
- [4] H. J. KIMBLE, M. DAGENAIS and L. MANDEL: *Phys. Rev. Lett.*, **39**, 691 (1977).
- [5] R. SHORT and L. MANDEL: *Phys. Rev. Lett.*, **51**, 384 (1983).
- [6] J. D. CRESSER, J. HAGER, G. LEUCHS, M. RATEIKE and H. WALTHER: *Topic in Current Physics*, Vol. 27, edited by R. BONIFACIO (Springer-Verlag, Berlin, 1982), p. 21.
- [7] M. C. TEICH and B. E. A. SALEH: *J. Opt. Soc. Am. B*, **2**, 275 (1985).
- [8] For a review, see: F. M. PIPKIN: *Adv. At. Mol. Phys.*, **14**, 281 (1978).
- [9] R. LOUDON: *The Quantum Theory of Light*, 2nd Edition (Clarendon, Oxford, 1983), p. 222.
- [10] A. ASPECT, P. GRANGIER and G. ROGER: *Phys. Rev. Lett.*, **47**, 460 (1981).
- [11] E. S. FRY: *Phys. Rev. A*, **8**, 1219 (1973).
- [12] B. E. A. SALEH and M. C. TEICH: *Opt. Commun.*, **52**, 429 (1985).
- [13] L. MANDEL: Communication at the Conference *New trends in Quantum Optics and Electrodynamics*, Roma, 1985.
- [14] E. JAKEMAN and J. G. WALKER: *Opt. Commun.*, **55**, 219 (1985).

## Observing the quantum behavior of light in an undergraduate laboratory

J. J. Thorn, M. S. Neel, V. W. Donato, G. S. Bergreen, R. E. Davies, and M. Beck<sup>a)</sup>

*Department of Physics, Whitman College, Walla Walla, Washington 99362*

(Received 4 December 2003; accepted 15 March 2004)

While the classical, wavelike behavior of light (interference and diffraction) has been easily observed in undergraduate laboratories for many years, explicit observation of the quantum nature of light (i.e., photons) is much more difficult. For example, while well-known phenomena such as the photoelectric effect and Compton scattering strongly suggest the existence of photons, they are not definitive proof of their existence. Here we present an experiment, suitable for an undergraduate laboratory, that unequivocally demonstrates the quantum nature of light. Spontaneously downconverted light is incident on a beamsplitter and the outputs are monitored with single-photon counting detectors. We observe a near absence of coincidence counts between the two detectors—a result inconsistent with a classical wave model of light, but consistent with a quantum description in which individual photons are incident on the beamsplitter. More explicitly, we measured the degree of second-order coherence between the outputs to be  $g^{(2)}(0) = 0.0177 \pm 0.0026$ , which violates the classical inequality  $g^{(2)}(0) \geq 1$  by 377 standard deviations. © 2004 American Association of Physics Teachers.

[DOI: 10.1119/1.1737397]

### I. INTRODUCTION

Students often believe that the photoelectric effect, and Einstein's explanation of it, proves that light is made of photons. This is simply not true; while the photoelectric effect strongly suggests the existence of photons, it does not demand it.<sup>1,2</sup> It was shown in the 1960s by Lamb and Scully that the photoelectric effect can be explained by assuming that the detector atoms are quantized, but that the field is not (i.e., by assuming light to be a classical wave). This explanation is based on the semiclassical model of photoelectric detection, which we will discuss further below.<sup>3,4</sup>

How then does one prove that photons exist? Here, we will assume that proving photons exist is equivalent to observing an effect that requires a quantum mechanical description of the field; equivalently, we will say that photons exist if the results of an experiment cannot be explained using a classical wave theory of light. Ideally, an experiment to prove the existence of photons will also demonstrate that light has “granular” properties. While physicists may argue about which specific experiment was the first to conclusively demonstrate the existence of a field requiring a quantum mechanical (QM) description, one can be fairly certain that this experiment was carried out in the 1970s.<sup>5–7</sup> While many such experiments have subsequently been performed, we know of very few that are well-suited for an undergraduate laboratory.<sup>8–10</sup>

In 1986, Grangier, Roger, and Aspect performed an elegant experiment.<sup>11,12</sup> Conceptually very simple, their approach was to examine correlations between photodetections at the transmission and reflection outputs of a 50/50 beamsplitter. To quote the experimenters, “a single photon can only be detected once!”<sup>11</sup> Hence, if a single quantum of light is incident on the beamsplitter (BS), it should be detected at the transmission output or at the reflection output, but not both: there should be no coincident detections between the two outputs. In fact, Grangier *et al.* measured fewer coincidences than predicted by a classical wave theory, violating a classical inequality by 13 standard deviations, and demonstrating that the field incident on the beamsplitter was well

described by a single-photon state.<sup>11</sup> As discussed below in more detail, the key challenge in such a measurement is to create a field that truly has a *single*-photon incident on the BS; a weak beam containing on *average* a single photon (or less) is not sufficient.

Here, we have repeated the experiment of Grangier *et al.*, adapting it for an undergraduate laboratory. We have taken advantage of over 15 years of technological advancements to obtain orders of magnitude increased count rates over those obtained by Grangier *et al.* The increased count rate in our experiment allows us to violate a classical inequality by 146 standard deviations with only 5 min of counting time. Our experiment is well described by the QM description of a field in a single photon state incident on a beamsplitter.

### II. HISTORY AND THEORY

#### A. Early measurements

As stated above, we are interested in examining correlations between the photocounts on two detectors situated at the output ports of a BS (Fig. 1). The first experiment to examine these correlations was carried out by Hanbury Brown and Twiss,<sup>13,14</sup> who found a positive correlation between the outputs of the two detectors. It should be noted that in this first experiment, Hanbury Brown and Twiss were not counting individual photons, but were instead measuring correlations between continuous currents from photomultiplier tubes (PMTs).<sup>13</sup> As such, this positive correlation indicated that when the current from one PMT increased, the current on the second tended to increase simultaneously. While the intent of Hanbury Brown and Twiss was to develop a new technique for measuring the angular diameter of stars,<sup>15</sup> their work played an important role in creating the field of quantum optics.

A brief controversy arose when Brannen and Ferguson performed a similar experiment in which they observed no positive correlation, and then claimed “that if such a positive correlation did exist, it would call for a major revision of some fundamental concepts in quantum mechanics.”<sup>16</sup> However, Purcell<sup>17</sup> and Hanbury Brown and Twiss<sup>18</sup> quickly

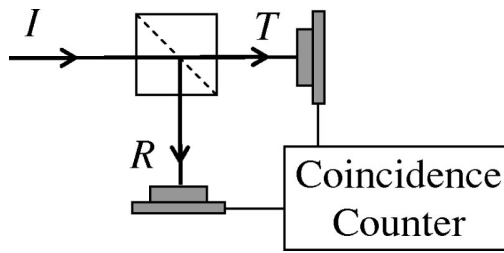


Fig. 1. Coincidence measurement. The incident ( $I$ ) beam is split into transmitted ( $T$ ) and reflected ( $R$ ) beams at a 50/50 BS. Detections at  $T$  and  $R$  are examined to see whether or not they occur simultaneously.

noted that the experimental parameters used by Brannen and Ferguson precluded the observation of positive correlations. They also showed that positive correlations are not only allowed by quantum mechanics, but are a natural consequence of the tendency for photons (and other bosons) to “bunch” together. The first experiment to observe positive correlations using coincidence detection of individual photocounts (not just photocurrents) from PMTs was performed by Twiss, Little, and Hanbury Brown,<sup>19</sup> who observed positive correlations of a few percent. This amount of correlation was consistent with that expected, given their experimental parameters.

## B. Classical fields

By a classical field, we mean an electromagnetic wave that is perfectly described by Maxwell’s equations. For such a field, the correlations between the intensities of the transmitted  $I_T$  and reflected  $I_R$  beams are given by the *degree of second-order (temporal) coherence*,  $g_{T,R}^{(2)}(\tau)$ , which is a function of the time delay  $\tau$  between the intensity measurements:<sup>20</sup>

$$g_{T,R}^{(2)}(\tau) = \frac{\langle I_T(t+\tau)I_R(t) \rangle}{\langle I_T(t+\tau) \rangle \langle I_R(t) \rangle}. \quad (1)$$

If the light source is *stationary* (i.e., if its statistics do not change in time), then we can interpret the brackets as referring to ensemble averages rather than time averages. It is called the degree of second-order coherence because it involves correlations between intensities, whereas the degree of first-order coherence describes correlations between fields.

Of particular importance to the present work is the case of simultaneous ( $\tau=0$ ) intensity measurements. In this case, and furthermore assuming a 50/50 BS in which the transmitted, reflected, and incident intensities are related by  $I_T(t) = I_R(t) = \frac{1}{2}I_I(t)$ , it is straightforward to see that

$$g_{T,R}^{(2)}(0) = g_{I,I}^{(2)}(0) = \frac{\langle [I_I(t)]^2 \rangle}{\langle I_I(t) \rangle^2} = g^{(2)}(0). \quad (2)$$

From the Cauchy–Schwartz inequality, it is straightforward to prove that  $\langle I_I(t) \rangle^2 \leq \langle [I_I(t)]^2 \rangle$ .<sup>20,21</sup> Using this, we find that

$$g_{T,R}^{(2)}(0) = g^{(2)}(0) \geq 1 \quad (\text{classical fields}), \quad (3)$$

where we emphasize that this result has been derived using classical wave theory. In Eq. (3), equality with 1 is achieved if the input field is perfectly stable with no fluctuations, while for fluctuating fields the second-order coherence is greater than 1. For “chaotic” light (e.g., light from a thermal

source that is either collisionally or Doppler broadened), it can be shown that  $g^{(2)}(0) = 2$ .<sup>20</sup> In an ingenious set of experiments involving a “pseudothermal” light source (a laser whose phase was randomized by a rotating ground-glass slide), Arrechi *et al.* were able to measure fields with  $g^{(2)}(0) = 1$  and  $g^{(2)}(0) = 2$ .<sup>22</sup>

## C. Semiclassical theory of photodetection

So far, we have been speaking about correlations between the intensities of the fields leaving the BS. In an experiment, however, one does not measure the intensity directly, but rather the photocurrent from a detector. It is then necessary to model the photodetection process. Since to this point we have been discussing classical fields, it is most appropriate to use a model that treats the field classically. The most rigorous theory of this sort is the semiclassical theory of photoelectric detection, in which the field is treated classically and the photodetector is treated quantum mechanically.<sup>23</sup> For the purposes of the discussion here, it is convenient to refer to the detector monitoring the transmitted (reflected) field as detector  $T$  ( $R$ ).

In the semiclassical theory of photoelectric detection, it is found that the conversion of continuous electromagnetic radiation into discrete photoelectrons is a random process. The probability of obtaining a single photocount from a single detector (for example, detector  $T$ ) within a short time window  $\Delta t$  is proportional to the average intensity of the field striking that detector, given as

$$P_T \Delta t = \eta_T \langle I_T(t) \rangle \Delta t, \quad (4)$$

where  $\eta_T$  is a constant that characterizes the detection efficiency of detector  $T$ . The joint probability of obtaining a photocount (within a time window  $\Delta t$ ) at detector  $R$ , and then after a time  $\tau$  obtaining a photocount at detector  $T$  (within a time window  $\Delta t$ ), is given by

$$P_{TR}(\tau) \Delta t^2 = \eta_T \eta_R \langle I_T(t+\tau)I_R(t) \rangle \Delta t^2. \quad (5)$$

It is then easily seen that if one measures the probability of joint and individual photocounts at detectors  $T$  and  $R$ , one can determine the degree of second-order coherence from

$$g_{T,R}^{(2)}(\tau) = \frac{P_{TR}(\tau)}{P_T P_R}. \quad (6)$$

Again, we are most interested in simultaneous,  $\tau=0$ , detection of photocounts at detectors  $T$  and  $R$ , which occurs with probability  $P_{TR}(0)$ . Using Eq. (3), we find that for classical fields, the measured degree of second-order coherence must be greater than or equal to 1:

$$g_{T,R}^{(2)}(0) = \frac{P_{TR}(0)}{P_T P_R} = g^{(2)}(0) \geq 1 \quad (\text{classical fields}). \quad (7)$$

Here, we see that if the joint probability factorizes,  $P_{TR}(0) = P_T P_R$ , which occurs when the detections at  $T$  and  $R$  are completely uncorrelated, then  $g^{(2)}(0)$  is minimized and is equal to 1.

We can summarize what we have learned about classical field statistics as follows. It is possible to measure the degree of second-order coherence between the fields leaving a beamsplitter  $g^{(2)}(0)$  by measuring the probability of joint and individual photocounts at detectors  $T$  and  $R$ . The second-order coherence must satisfy the inequality  $g^{(2)}(0) \geq 1$ .

When the photocounts at  $T$  and  $R$  are completely uncorrelated,  $g^{(2)}(0)=1$ , which occurs when the input field to the beamsplitter is a perfectly stable wave. If the input field fluctuates, then  $g^{(2)}(0)>1$ , indicating positive correlations between the photocounts.

Since  $g^{(2)}(0)$  cannot be less than 1, we are left with the conclusion that for classical fields the measured photocounts at  $T$  and  $R$  cannot be anticorrelated. This makes sense because a BS simply splits a classical input field into two identical copies. These output fields either fluctuate together (positive correlation) or do not fluctuate at all (no correlation). It is not possible for the intensity of one to decrease while the intensity of the other increases (anticorrelation).

#### D. Quantum fields

From the time of the original Hanbury Brown and Twiss experiment in 1956,<sup>13</sup> the importance of a rigorous theory of photoelectric counting was recognized. The first attempts were the semiclassical theories discussed in the previous section. In the mid-1960s sophisticated fully QM theories, in which both the electromagnetic field and the detector atoms are treated quantum mechanically, were developed by Kelly and Kleiner,<sup>24</sup> Glauber,<sup>25</sup> and others (see Refs. 20 and 23, and the references therein). A QM field is not fully described by Maxwell's equations.

In the fully quantum theory, the correlations between the output fields from the BS in Fig. 1 are still described by the degree of second-order coherence  $g_{T,R}^{(2)}(\tau)$ , although now the electric fields (and corresponding intensities) are treated as QM operators, rather than as classical waves. Again, we are interested in simultaneous ( $\tau=0$ ) detection of photons at the outputs; quantum mechanically  $g_{T,R}^{(2)}(0)$  is defined as

$$g_{T,R}^{(2)}(0) = \frac{\langle : \hat{I}_T \hat{I}_R : \rangle}{\langle \hat{I}_T \rangle \langle \hat{I}_R \rangle}. \quad (8)$$

Here the colons indicate that the creation  $\hat{a}^\dagger$  and annihilation  $\hat{a}$  operators corresponding to the electric fields are to be placed in normal order, which means that all creation operators appear to the left of all annihilation operators. The intensity operator is proportional to the photon number operator for the field  $\hat{n} = \hat{a}^\dagger \hat{a}$ , so that

$$g_{T,R}^{(2)}(0) = \frac{\langle : \hat{n}_T \hat{n}_R : \rangle}{\langle \hat{n}_T \rangle \langle \hat{n}_R \rangle} = \frac{\langle \hat{a}_T^\dagger \hat{a}_R^\dagger \hat{a}_R \hat{a}_T \rangle}{\langle \hat{a}_T^\dagger \hat{a}_T \rangle \langle \hat{a}_R^\dagger \hat{a}_R \rangle}, \quad (9)$$

where we have explicitly placed the field operators in normal order.

The averages in Eqs. (8) and (9) are given by QM expectation values. The expectation value is computed using the field states at the detectors. These states can be derived from the input state to the BS.<sup>23,26</sup> Alternatively, the operators for the reflected and transmitted fields can be written in terms of the operators for the input field  $\hat{a}_I$ , and the unoccupied (vacuum) field  $\hat{a}_V$  that enters the unused port of the BS (Fig. 2). For a 50/50 BS, and one particular choice of phase for the BS, it is straightforward to show that

$$\hat{a}_R = \frac{1}{\sqrt{2}}(\hat{a}_I + \hat{a}_V), \quad \hat{a}_T = \frac{1}{\sqrt{2}}(\hat{a}_I - \hat{a}_V). \quad (10)$$

Substituting the reciprocity relations Eq. (10) into Eq. (9), and using the fact that the unoccupied field mode is in a

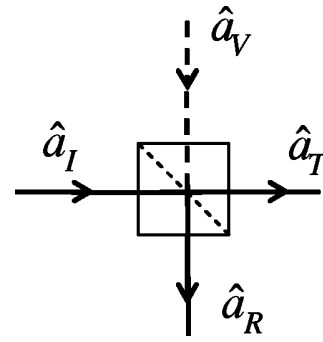


Fig. 2. Field operators corresponding to BS input and output ports.

vacuum state, the second-order coherence can be rewritten as<sup>20</sup>

$$g_{T,R}^{(2)}(0) = \frac{\langle \hat{n}_I(\hat{n}_I - 1) \rangle}{\langle \hat{n}_I \rangle^2} = g_{I,I}^{(2)}(0) = g^{(2)}(0), \quad (11)$$

where now the expectation value is computed using the QM state of the field incident on the BS. As in the classical case, the second-order coherence between the BS outputs is equal to the second-order coherence of the input.

Quantum mechanically, the measured correlations at the detectors are determined by the state of the field incident on the BS (the input state). The QM equivalent to a stable classical wave is a coherent state  $|\alpha\rangle$ , which is the eigenstate of the annihilation operator  $\hat{a}|\alpha\rangle = \alpha|\alpha\rangle$ .<sup>20</sup> If one evaluates the second-order coherence [Eq. (11)], assuming an input field in a coherent state, one finds  $g^{(2)}(0)=1$ , which is the same as the classical result for a stable classical wave. Evaluating Eq. (11) assuming an input field in a thermal state (which is an incoherent mixture described by a density operator) one finds  $g^{(2)}(0)=2$ .<sup>20</sup> Such a field is said to be ‘‘bunched,’’ because one interpretation of this result is that the photons tend to come in bunches; once they strike the BS, some are transmitted and others are reflected, leading to positive correlations between the output fields.

Thus, the quantum theory of photoelectric detection is in agreement with the classical theory described in Sec. II, as long as one uses the appropriate field states. However, there exist certain field states that are inherently QM in nature, and for which there is no classical wave theory counterpart. Such nonclassical fields are not in general constrained by the limits discussed in Sec. II C. An example of a nonclassical field state is one containing exactly one photon; this state is an eigenstate of the photon number operator, with eigenvalue 1:  $\hat{n}|1\rangle = 1|1\rangle$ . Evaluating Eq. (11) using an input field in a single-photon state yields  $g^{(2)}(0)=0$ , which violates the classical inequality  $g^{(2)}(0) \geq 1$ .

Theoretically predicting the existence of nonclassical fields, and generating them in the laboratory, however, are two very different matters. One of the first experiments to demonstrate the existence of a nonclassical field was performed by Kimble, Dagenais, and Mandel in 1977.<sup>7</sup> They measured the light emitted by a single atom (‘‘resonance

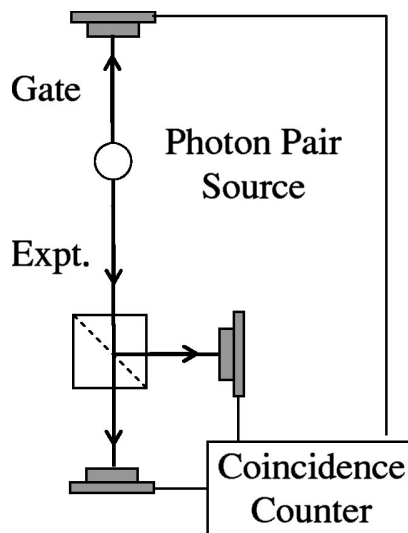


Fig. 3. Coincidence measurements with a gate. A source emits pairs of photons simultaneously, and the photons travel in opposite directions. Detection of the gate signal tells the  $T$  and  $R$  detectors when to expect a “proper” detection on the experiment side.

fluorescence”) and found  $g^{(2)}(0) = 0.4 \leq 1$ , proving that the field was “anti-bunched.” An anti-bunched field can be interpreted as one in which the photons do not clump together, and hence tend to arrive one at a time. When these individual photons strike the beamsplitter, they are either transmitted or reflected (but not both), leading to anticorrelations in the photocounts at the detectors.

Despite clearly demonstrating that the light emitted by a single atom is anti-bunched, this experiment was complicated by the difficulty of isolating the light coming from the atom from the background scattered light. This complication was due to the fact that the laser light used to excite the atom and the resonance fluorescence were both at the same frequency. To isolate the resonance fluorescence, it was necessary to use a detailed model of the experiment, and to correct for the expected contribution from the scattered laser light.

A conceptually much simpler demonstration of photon anti-bunching was performed by Grangier, Roger, and Aspect in 1986.<sup>11</sup> A schematic of their experiment is shown in Fig. 3. They circumvented the problem of background light by using a two-photon cascade in Ca. In this process, a Ca atom absorbs two photons, one each from two lasers operating at frequencies  $\nu_{11}$  and  $\nu_{12}$ , promoting it to an excited state. The Ca atom then decays by emitting two photons at different frequencies: one at frequency  $\nu_1$  by decaying to a short-lived intermediate level, and a second at frequency  $\nu_2$  by decaying to the ground state. All four frequencies are distinct and can be isolated using filters, greatly reducing the problem of scattered background from the intense laser beams. Furthermore, angular momentum conservation ensured that the two photons always were emitted in opposite directions. The detection of one photon at one detector ensured that there would be a photon heading in the opposite direction, so that the first photon could be used as a gate to tag the arrival of the second. Thus, when a gate photon was detected, it was known with high confidence that there was one (and only one) photon incident on the BS.

For this experiment, detections at  $T$  and  $R$  were condi-

tioned upon detections at the gate detector (detector  $G$ ). With this conditioning, the measured degree of second-order coherence [Eq. (6)] is given by

$$g^{(2)}(0) = \frac{P_{GTR}}{P_{GT}P_{GR}}. \quad (12)$$

Here,  $P_{GT}$  ( $P_{GR}$ ) is the probability of measuring simultaneous photocounts at detector  $T$  ( $R$ ) and detector  $G$ , and  $P_{GTR}$  is the probability of obtaining a threefold coincidence between detectors  $T$ ,  $R$ , and  $G$ . The probabilities can be written as

$$P_{GTR} = \frac{N_{GTR}}{N_G}, \quad P_{GT} = \frac{N_{GT}}{N_G}, \quad P_{GR} = \frac{N_{GR}}{N_G}, \quad (13)$$

where, given a specified time window,  $N_{GT}$  ( $N_{GR}$ ) is the number of simultaneous photocounts at detector  $T$  ( $R$ ) and detector  $G$ ,  $N_{GTR}$  is the number of threefold coincidences, and  $N_G$  is the number of singles counts at detector  $G$ . By using Eq. (13), we can rewrite the experimentally determined degree of second-order coherence [Eq. (12)], as

$$g^{(2)}(0) = \frac{N_{GTR}N_G}{N_{GT}N_{GR}}. \quad (14)$$

In an experimental tour-de-force, Grangier *et al.* measured a second-order coherence of  $g^{(2)}(0) = 0.18 \pm 0.06$ , which violated the classical inequality  $g^{(2)}(0) \geq 1$  by 13 standard deviations.<sup>11</sup> In a 5 h experiment, they measured a total of nine threefold coincidences, while a classical wave theory would have predicted greater than 50 threefold coincidences. If the state were a perfect one-photon state, Grangier *et al.* would have measured no threefold coincidences.

We have repeated the experiment of Grangier *et al.*; with advances in technology over the past 15+ years, however, a tour-de-force is no longer required. By using only readily available, off-the-shelf components, we were able to assemble this experiment in an undergraduate laboratory. In a typical run lasting less than 5 min, we measure  $g^{(2)}(0) = 0.0188 \pm 0.0067$ , where no corrections have been applied to the data to account for accidental coincidences. We have also determined that by accounting for the expected accidental coincidences (see Appendix A), the difference between our result and  $g^{(2)}(0) = 0$  (i.e., that expected from a true single-photon incident on the BS) is fully explained by the accidental coincidences.

### III. PARAMETRIC DOWNCONVERSION

The key to our ability to perform the experiment is our use of a parametric down-conversion source in place of the atomic Ca cascade source used by Grangier *et al.*<sup>11</sup> This method has the advantages of increased simplicity, reduced cost, and increased count rates (several orders of magnitude greater than those observed by Grangier *et al.*) In the process of spontaneous parametric downconversion, a single photon of one frequency is converted into two photons of lower frequency (by approximately a factor of 2). Although down-conversion is extremely inefficient (milliwatts of input power generate output beams that must be detected using photon counting), it is much more efficient than the Ca cascade.

The input is referred to as the pump (at angular frequency  $\omega_p$ ), while the two outputs are referred to as the signal and idler (at angular frequencies  $\omega_s$  and  $\omega_i$ ). Energy conservation requires that

$$\hbar \omega_p = \hbar \omega_s + \hbar \omega_i, \quad \omega_p = \omega_s + \omega_i. \quad (15)$$

Momentum conservation is equivalent to the classical phase-matching condition, which requires that the wave vectors of the input and output fields satisfy

$$\vec{k}_p = \vec{k}_s + \vec{k}_i. \quad (16)$$

The frequencies and wave vectors are not independent of each other, and are related by the dispersion relation

$$k_p = \frac{n_p(\omega_p)\omega_p}{c}, \quad (17)$$

where  $n_p(\omega_p)$  is the index of refraction of the pump wave at the pump frequency, and similarly for the signal and idler waves.

In Type-I downconversion, which is what we use in our experiments, the signal and idler beams are polarized parallel to each other, and their polarization is perpendicular to that of the pump; all polarizations are linear. By proper orientation of the pump beam wave vector  $\vec{k}_p$  with respect to the optic axis of the crystal, it is possible to satisfy the constraints imposed in Eqs. (15)–(17). Because only the relative angle between the pump, signal, and idler are important, the downconverted light is emitted into a cone surrounding the pump beam (see, for example, Ref. 9).

Typically, the frequencies of the signal and idler beam are chosen to be equal to each other, at half the frequency (twice the wavelength) of the pump. In order to separate the signal and idler, they are chosen to make a small angle (a few degrees) with the pump beam so that the signal comes out a few degrees from the pump, and the idler comes out a few degrees on the other side of the pump.

However, for a given crystal orientation, there is no unique solution to the constraints imposed in Eqs. (15)–(17). The sums of the frequencies and wave vectors are constrained, but not the individual frequencies and wave vectors. For instance, if the signal frequency is less than half the pump frequency by a certain amount, it is possible for energy to be conserved [Eq. (15)], if the idler frequency is an equal amount greater than half the pump frequency. In order for momentum to be conserved [Eq. (16)], the signal makes a slightly greater angle with respect to the pump, and the idler makes a slightly smaller angle. Thus, the light coming out of a downconversion crystal is emitted into a range of angles (several degrees), and wavelengths (on the order of 10s of nm, centered about twice the pump wavelength).

The similarity between the Ca cascade source used by Grangier *et al.*<sup>11</sup> and our downconversion source is that both sources produce two photons, one of which is used as a gate. In our experiment, we use the idler photons as a gate—the detection of an idler photon in one beam (using detector  $G$ ) indicates that there is a signal photon present in the other. The signal beam is directed to a beamsplitter with two detectors at its outputs (detectors  $T$  and  $R$ ). Just as in the experiment of Grangier *et al.*, we expect to see an absence of coincidences between the  $T$  and  $R$  detectors, conditioned on a detection at  $G$ . This absence is equivalent to an absence of threefold coincidences between  $G$ ,  $T$ , and  $R$ . We can use Eq.

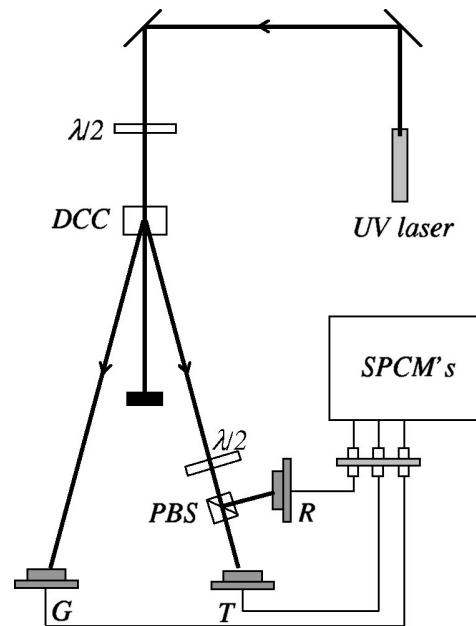


Fig. 4. Experimental apparatus. Major components include an ultraviolet laser, downconversion crystal (DCC), polarizing beamsplitter (PBS), single-photon counting modules (SPCMs), and gating, transmission-side, and reflection-side collection optics ( $G, T, R$ ). Optical fibers direct the light from  $G$ ,  $T$ , and  $R$  to their corresponding SPCMs.

(14) as a measure of the second-order coherence of the signal beam, and a result of  $g^{(2)}(0) < 1$  is inconsistent with a classical wave description of our system.

#### IV. EXPERIMENT

We now describe the major components for our updated version of the experiment of Grangier *et al.* The layout of these components is presented in Fig. 4. In brief, a beam of ultraviolet laser light enters a nonlinear crystal where, via spontaneous parametric downconversion, some of the light is converted into IR light in two beams. Light from one of the IR beams (the idler) is used as a *gating beam* and passes directly from the crystal into a photodetector. Light from the other beam (the signal), which we shall call the *experiment beam*, is directed into a 50/50 BS and subsequently observed by photodetectors placed in both the transmission and reflection ports of the beamsplitter. A photodetection in the gating beam is used to signal that the experiment beam has been prepared in the proper single-photon state, and it is the light in the experiment beam whose second-order coherence is measured. Detections from the three detectors  $G$ ,  $T$ , and  $R$  are registered by a series of time-to-amplitude converters and single-channel analyzers; coincidence statistics are then compiled and analyzed.

For a more detailed discussion, it is convenient to group components of the instrument into three categories: (i) light source, (ii) light detection, and (iii) coincidence-counting electronics; there also are some diagnostic instruments that make the experiments easier to perform. A list of major components, manufacturers, and part numbers is provided in Appendix C; all of the equipment is commercially available and relatively affordable; a complete parts list and further information is available on our website.<sup>27</sup>

### A. Light source

Our light source was designed to be sufficiently bright so that alignment can be done in real time; we obtain sufficient coincidences in a 100-ms counting window to use the  $\sim 10$ -Hz rate of raw coincidence measurements to perform final alignment. Given this high brightness, data collection occurs over a few minutes (our experimental runs last from approximately 5 to 40 min).

The pump laser used in this work is a cw ultraviolet (409 nm), diode-pumped, frequency-doubled, solid-state laser; the pump is linearly polarized. It was chosen for its turnkey operation, high output power (20 mW), long advertised lifetime (10 000 h) and comparative value. Before entering the downconversion crystal, the pump passes through a zero-order, 400-nm half-wave plate, which allows us to adjust the pump polarization to maximize the downconversion rate (by rotating a half-wave plate in its mount, the direction of linear polarization also rotates.) Downconversion is accomplished in a  $5 \times 5$  mm aperture, 3-mm-long beta-barium borate (BBO) crystal. It is cut for Type-I downconversion of 405-nm pump light, with a 810-nm signal and idler waves making angles of  $\theta = 3^\circ$  with respect to the pump. Because the crystal is hygroscopic, the crystal faces have humidity-barrier, antireflective coatings. The crystal is mounted so that a small flow of dry nitrogen flows over it while in use on the optical table. When not in use, the crystal is stored in a desiccant jar.

When discussing the performance of the source, it is useful to talk in terms of the count rates  $R$ , measured in counts per second (cps);  $R_G = N_G / \Delta T$ , where  $\Delta T$  is the measurement time, and similarly for other count rates. Our source regularly produces singles count rates in the signal and idler beams (e.g.,  $R_G$ ) of  $\sim 110\,000$  cps, and total coincidence rates between the signal and idler beams of  $\sim 8800$  cps (coincidence rates for the counters behind the BS,  $R_{GT}$  and  $R_{GR}$  are half this value.)

The downconverted light is vertically polarized. Instead of using an ordinary 50/50 BS, we use a combination of a half-wave plate and a polarizing beamsplitter (PBS). The half-wave plate is adjusted so that the light entering the PBS is polarized at  $45^\circ$  with respect to the polarization axis of the PBS; the light then splits equally between the two outputs. By rotating the half-wave plate, we can adjust the input polarization (and hence the splitting ratio), allowing us to fine tune the splitting to be as close to 50/50 as possible. We also can easily transmit or reflect 100% of the beam, which is useful during alignment.

### B. Light detection

Our light collection optics are designed for ease of alignment and ambient light rejection. The use of fiber optic cables also makes the system very flexible. We highly recommend that anyone performing experiments with downconverted light consider using a similar fiber-based system.

The collection optics and detection systems for the three detectors ( $G$ ,  $T$ , and  $R$ ) are identical. Downconverted light is collected by a converging lens and focused into the end of a  $62.5\text{-}\mu\text{m}$ -diameter, 1-m-long multimode fiber optic cable that has fiber-coupling (FC) connectors on both ends. The lens is a fiber-coupling lens (Thorlabs F220FC-B), and is pre-aligned to place the tip of the fiber cable in the focal plane of the lens, so that no alignment of the lens to the fiber is necessary. The other end of the fiber connects to a fiber-to-

fiber coupler, which couples light into a second, identical, fiber. This arrangement allows us the flexibility of swapping connections between the coupling lenses and different detectors, which is useful in setting up the coincidence counting electronics (detailed below). It also allows us to easily connect a fiber-coupled laser diode which shines light backward through the coupling lens onto the downconversion crystal for alignment purposes (detailed below). The second fiber carries the downconverted light into a light-tight enclosure which houses the optical filters and detectors. The only light entering this enclosure comes through the fibers, which greatly eliminates problems with stray light.

Light is coupled out of the second fiber with another fiber-coupling lens, passes through an RG 780 filter (which passes wavelengths longer than 780 nm), and is coupled with a third lens into a third fiber cable ( $50\ \mu\text{m}$  diameter, FC connectors, and an opaque jacket). We use a kinematic mount to align the output of one lens with the input of the other. We also surround the lenses and filter with beam tubes to further eliminate the possibility of collecting ambient light. The third fiber cable transports the light to the single-photon counting module (SPCM), which has its own FC connector which is pre-aligned to image the fiber tip onto the active area of the detector.

The SPCMs use an avalanche photodiode operated in Geiger mode to detect the light. They output a 30 ns, 4.5 V (into  $50\ \Omega$ ) pulse when they detect a photon, with a 50 ns dead time between pulses. The SPCMs have a specified quantum efficiency of  $\sim 50\%$  at 810 nm, and the model we used had dark count rates of  $\sim 250$  cps. With this dark count rate and our 2.5-ns coincidence window, coincidences due to dark counts are negligible.

### C. Coincidence counting electronics

As described above, we are interested in detecting coincidence counts between the outputs of different detectors. We use a coincidence window of 2.5 ns, and coincidences are determined using a combination of a time-to-amplitude converter (TAC) and a single-channel analyzer (SCA). Three such coincidence units are used (one each for  $GT$ ,  $GR$ , and  $GTR$  coincidences), and their outputs are recorded by a counting board in our computer. We briefly describe how we use the TAC/SCA to determine twofold  $GT$  coincidences. ( $GR$  coincidences are determined in the same manner). Modification of the TAC/SCA configuration to obtain threefold  $GTR$  coincidences also is described.

A TAC operates by receiving two inputs, called START and STOP, and then outputting a pulse, the amplitude of which is proportional to the time interval between the rising edges of the START and STOP signals. The proportionality between the amplitude and the time interval is controlled by the gain of the TAC, and we typically use a value of 0.2 V/ns. To measure  $GT$  coincidences, the START input comes from the output of detector  $G$  and the STOP input comes from detector  $T$  (see Fig. 5). To ensure that the START pulse precedes the STOP pulse, we insert an extra length of coaxial cable, corresponding to a delay of  $\sim 6$  ns, between  $T$  and the STOP input. Thus, if detectors  $G$  and  $T$  record simultaneous detections, the delay between START and STOP signals is 6 ns, and the output from the TAC is 1.2 V.

The SCA operates by receiving an input pulse, and then outputting a pulse (with an amplitude of 5 V) *only* if the amplitude of the input pulse falls within a certain voltage window. The width of the window is adjustable, as is the

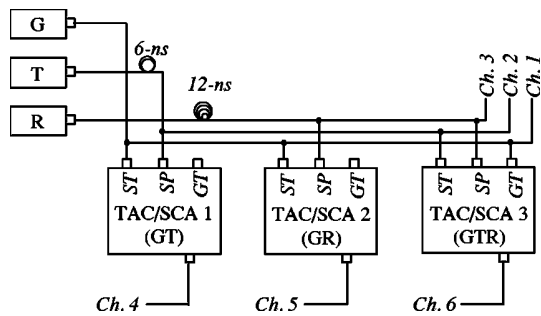


Fig. 5. Coincidence counting electronics. TACs and SCAs are used to identify  $GT$ ,  $GR$ , and  $GTR$  coincident detections. Here  $ST$ ,  $SP$ , and  $GT$  refer to START, STOP, and START GATE inputs, respectively. The outputs go to six input channels on the counter.

lower level of the window. The input to the SCA is the output from the TAC. Using the values for the TAC output above, a coincidence window of 2.5 ns centered about 6 ns corresponds to a voltage range of 0.95–1.45 V, and our SCA is configured to output a pulse if the amplitude of the input pulse lies within this range. The only trick to configuring the TAC/SCA setup is in properly setting the SCA window to maximize true coincidences and reject false coincidences. This procedure is described in Appendix B.

In order to measure the threefold  $GTR$  coincidences, we use  $T$  as the START input and  $R$  as the STOP input, and configure the TAC/SCA as described above to register  $TR$  coincidences. To ensure that these  $TR$  coincidences also are coincident with a detection at  $G$ , we operate the TAC in “start gate coincidence” mode, and feed the  $G$  signal to the START GATE input of the TAC. If an output pulse from  $G$  is not present at the START GATE when the pulse from  $T$  arrives at START, then the timing circuitry in the TAC is disabled, and no output is produced.

There is one last trick used in setting up this threefold coincidence unit. The technique for setting the SCA window described in Appendix B relies on observing coincidences between the detectors measuring the START and STOP input; however, we expect an *absence* of coincidences between  $T$  and  $R$ . In order to obtain coincidences between these detectors so that we can set the window, we switch the fiber optic cables so that the idler (gate) beam is fed into the detector that ordinarily measures the  $R$  output. Now, we have coincident photons entering the two detectors, so that we can set the window as described in Appendix B. The delays are all set by the coaxial (electrical) cables between the detectors and the coincidence units. Because all of the fiber cables have the same length, the optical delays are the same, and switching the fiber cables back after the window is set does not affect the timing.

We measure a total of six photocounts in each data acquisition interval: singles counts from each of the three detectors,  $N_G$ ,  $N_R$ , and  $N_T$ , as well as the coincidence counts  $N_{GR}$ ,  $N_{GT}$ , and  $N_{GTR}$ . We use a counting board that plugs into a PCI slot in our computer, and it simultaneously records these counts on six different channels. A LABVIEW program reads the data from the board, computes the second-order coherence [Eq. (14)], and saves the data.

## D. Optical alignment

Although requiring some care, we have found the setup and alignment process to be sufficiently straightforward that two undergraduates having some familiarity with the experiment were able to start from a bare optical table and complete the process with minimal supervision over the course of one or two days. The alignment is robust once it has been completed. For example, we remove the downconversion crystal when it is not in use; reinserting the crystal and tweaking-up the alignment takes only a few minutes. When starting from scratch, the major components are first affixed to the optical table in rough alignment as illustrated in Fig. 4; although at first we are interested solely in obtaining coincidences between the idler and signal beams, so that the half-wave plate, PBS, and detector  $R$  are not used. The pump beam is aligned level to the table using the two mirrors, and the electrical connections are completed.

The first component to be aligned is the collection optics (i.e., fiber optic cable/lens assembly) for the  $G$  detector. The collection lens is mounted in a kinematic mount that allows for horizontal, vertical, and angular adjustment, and the center height of the lens is adjustable using a post holder and post. The height is initially adjusted so that the center of the lens is at the same height as the pump beam. Light from a fiber-coupled 780 nm laser diode is coupled (via the fiber-to-fiber coupler) backward through the fiber cable, and out through the lens. The lens is placed so that angle of this beam is set to be  $3^\circ$  off of the pump beam, and the mount is adjusted so that the laser shines back onto the center of the downconversion crystal. The alignment laser is now removed and the fiber cable is connected to the detector. By monitoring the count rate from the  $G$  detector, the polarization of the pump and the horizontal and vertical tilt of the downconversion crystal are adjusted to maximize the count rate. Once this adjustment has been accomplished, the kinematic mount controlling the alignment of the two lenses surrounding the RG780 filter also is adjusted to maximize the count rate. Now, the horizontal placement of the collection lens (and hence the angle between the collection lens and the pump beam) is carefully adjusted to maximize the count rate. The alignment of the downconversion crystal and placement of the collection beam is then iterated to maximize the count rate on the  $G$  detector. As stated above, we typically obtain  $\sim 100\,000$  cps on this beam.

Next, the  $T$  detector is aligned in nearly the same way. At first the goal is not to painstakingly align this detector for maximum counts, but simply to get enough counts so that the coincidence window between the  $G$  and  $T$  detectors can be set as described in Appendix B. Once this alignment is set, the alignment of the  $T$  collection optics is adjusted to maximize the *coincidence* rate between  $G$  and  $T$ , not the raw count rate on  $T$ . We easily obtain a coincidence rate of over 7000 cps, and frequently achieve a rate of  $\sim 8800$  cps. Once the alignment of the  $T$  optics has been accomplished, the alignment laser is shone backward through this optics, and adjustable iris diaphragms are aligned with the beam in between the downconversion crystal and the  $T$  optics. These irises serve to identify the beam path and assist in aligning the  $R$  detector.

The half-wave plate and PBS are now inserted, and the alignment laser is shone backward through the collection optics of the  $R$  detector. The optics are adjusted so that the light goes back through the irises and onto the crystal. The  $R$  detector is connected and when counts are achieved, the win-

Table I. Measurements of  $g^{(2)}(0)$ , the degree of second-order coherence.

Trial (Total acquisition time, min)	Integration time per point (s)	Number of points	$g^{(2)}(0)$	Standard deviation of $g^{(2)}(0)$
1 (~5)	2.7	110	0.0188	0.0067
2 (~10)	5.4	108	0.0180	0.0041
3 (~20)	11.7	103	0.0191	0.0035
4 (~40)	23.4	100	0.0177	0.0026

dow on the  $GR$  coincidence unit is set, and the  $GR$  coincidence count is maximized. Lastly, the  $GTR$  coincidence unit is configured using the procedure described above.

## V. RESULTS

One of the primary advantages of the apparatus described in this paper is the ability to acquire good counting statistics in time periods reasonable for an undergraduate laboratory. In Table I, we present the results of four experimental runs. In each of these runs, we performed  $\sim 100$  measurements of  $g^{(2)}(0)$ , while in each run we changed the integration time for each measurement. These results are clearly inconsistent with a classical wave theory, which predicts  $g^{(2)}(0) \geq 1$ . Even for counting times of less than 5 min, we obtain a value of  $g^{(2)}(0)$  that is lower than the classical lower limit by 146 standard deviations. Increasing the counting time does not affect the measured value of  $g^{(2)}(0)$  (to within the statistical error of our measurement), but increasing the counting time does decrease the statistical error. Our best results is  $g^{(2)}(0) = 0.0177 \pm 0.0026$ , which violates the classical inequality by 377 standard deviations.

If a truly single-photon state were incident on the BS, QM would predict that  $g^{(2)}(0) = 0$ . Why don't we see this? A consequence of defining a "coincidence" with a finite time window is an expected nonzero anticorrelation parameter. This is because there is the possibility that uncorrelated photons from different downconversion events may hit the  $T$  and  $R$  detectors within our finite coincidence window; these are "accidental" coincidences. As the count rates and coincidence window increase, so do the number of accidental coincidences. In Appendix A, we analyze the effect of these accidental coincidences on our measurements of  $g^{(2)}(0)$ . For our experimental parameters, when we account for accidental coincidences, we calculate an expected value of the second-order coherence  $g^{(2)}(0) = 0.0164$ , which is what we observe to within our statistical error.

As a final check on the instrument and method, the measurement was repeated, but with an extra length of coaxial cable (corresponding to a delay of 6 ns) placed after the  $R$  detector. In this case we are not measuring true coincidences, but instead coincidences between measurements made at time  $t$  at detector  $R$ , and time  $t + 6$  ns for detector  $T$ . This means we do not measure the quantity  $g^{(2)}(\tau = 0)$ , but instead we measure  $g^{(2)}(\tau = 6 \text{ ns})$ . Under such circumstances,  $GTR$  coincidences are not excluded because we expect the detections at  $T$  and  $R$  to be due to uncorrelated downconversion events. Indeed, we would expect to obtain a measured

value  $g^{(2)}(\tau = 6 \text{ ns}) \geq 1$ . In two different experimental runs we obtained measured values for  $g^{(2)}(\tau = 6 \text{ ns})$  in the range 2–3.

## VI. CONCLUSIONS

We have performed an experiment whose results cannot be explained using a classical wave description for light. The results are consistent with a quantum mechanical description in which a field in a single-photon state is incident on a beamsplitter, and as such we take this experiment as proof of the existence of photons. The experiment is conceptually simple, and is suitable for an undergraduate laboratory.

While we would not describe the cost of this experiment as inexpensive (total cost of  $\sim \$40,000$ ), the cost is not prohibitive; a more detailed discussion of this cost is presented in Appendix C, along with the parts list. Furthermore, the equipment is extremely versatile and can be used for a number of other experiments. By adding approximately  $\$2,500$  in components, we have extended the work described here to demonstrate that (i) single photons interfere with themselves as they pass through the two arms of an interferometer, and (ii) that the frequencies of the signal and idler beams generated in our experiment are highly correlated. These experiments will be described in a future publication. With other small additional purchases, it will be possible to perform tests of Bell's inequalities<sup>9,10</sup> and to demonstrate two-photon interference.<sup>28,29</sup> Thus, for less than  $\$50,000$ , one could implement five experiments suitable for undergraduates that demonstrate interesting features of quantum mechanics. While the total cost is not inexpensive, it is most certainly cost effective.

## ACKNOWLEDGMENTS

We wish to acknowledge several helpful discussions with David Branning. We also acknowledge financial support from the National Science Foundation and from Whitman College.

*Note added in proof.* We have recently become aware that similar experiments have been carried out by a group at Colgate University.<sup>30</sup>

## APPENDIX A: ACCIDENTAL COINCIDENCES

The time interval defining a coincidence is determined by the windowing of the SCAs. Specifically, the SCAs are configured with finite time windows of  $\Delta t = 2.5 \text{ ns}$ , giving the term "coincidence" the meaning "within 2.5 ns". A consequence of this finite window is a finite probability, proportional to  $\Delta t$ , of registering  $GTR$  coincidences that have no relation to the coincidences of interest; these are accidental coincidences.

For example, suppose we obtain a valid coincidence between detectors  $G$  and  $T$ , which occurs with probability  $P_{GT} = R_{GT}/R_G$ , where we have written Eq. (13) in terms of the count rates. Within  $\Delta t$  of this coincidence, there is a random chance that the  $R$  detector also will measure a count, leading to an accidental threefold coincidence. If the time interval  $\Delta t$  is small enough, then the probability of this random  $R$  detection occurring can be approximated by  $P'_R \approx R_R \Delta t$ , where the prime indicates that this is an accidental event, occurring within a specific time window. Similarly, a valid  $GR$  coincidence and a chance detection at  $T$  also will

yield an accidental threefold coincidence. The probability of the accidental coincidences can then be written as

$$P'_{GTR} = P_{GT}P'_R + P_{GR}P'_T = P_{GT}R_R\Delta t + P_{GR}R_T\Delta t. \quad (18)$$

Here, we have ignored the probability that the accidental threefold coincidences may be due to pure chance detections at all three detectors, because for our count rates and coincidence window, this probability is negligible.

We can now calculate the effect of these accidental coincidences on the second-order coherence. Substituting Eq. (18) into Eq. (12) yields

$$\begin{aligned} g^{(2)}(0) &= \frac{P_{GTR}}{P_{GT}P_{GR}} \\ &= \frac{P_{GT}R_R\Delta t + P_{GR}R_T\Delta t}{P_{GT}P_{GR}} \\ &= \frac{R_R\Delta t}{P_{GR}} + \frac{R_T\Delta t}{P_{GT}} = R_G\Delta t \left( \frac{R_R}{R_{GR}} + \frac{R_T}{R_{GT}} \right). \quad (19) \end{aligned}$$

Using the average count rates obtained from the data collected during trial 4 of Table I, we calculate the contribution to  $g^{(2)}(0)$  from the accidental coincidences to be 0.0164.

## APPENDIX B: SETTING THE SINGLE-CHANNEL-ANALYZER WINDOW

One technique for setting the voltage window of the SCA is to simply set the window width to some value, and to slowly adjust the lower level of the window while monitoring the SCA output. The goal is to maximize the coincidence rate. The window is then adjusted to be just wide enough so that a further increase in width does not significantly increase the count rate. Adjustments of the width and lower level of the window can be iterated to optimize the count rate.

An easier way to set the SCA window is to use a multi-channel analyzer (MCA). Our MCA is on a PCI card that plugs into our computer and comes with its own software. We use it as a diagnostic tool for setting the window, but do not use it in our experiments to determine  $g^{(2)}(0)$ . An MCA histograms voltage pulses of varying amplitude. The histogram is displayed in real time, with an update rate of a few hertz, so that one can watch the histogram build over time. The input to the MCA is the output from the TAC, so that the histogram can be interpreted as measuring time intervals instead of voltages. As stated above, coincidence counts at  $G$  and  $T$  are separated at the TAC by 6 ns, and with the coincidence rates in our experiment, we easily see a peak in the histogram generated by the MCA centered at this 6-ns time delay. The wings of this peak extend outward to a width of approximately 2.5 ns, which is the reason we chose this value for our coincidence window. (This width is due almost entirely to the properties of the SPCMs, as the time interval between the photon pairs produced in our experiment is certainly much less than this.<sup>31</sup>) Uncorrelated photodetections (arising from  $G$  seeing a photon from one pair-production event and  $T$  seeing a photon from a different pair-production event) contribute a uniform background that the coincidence peak sits on top of.

Simply looking at the output of the TAC on the MCA displays the coincidence peak, but yields no information about the window of the SCA, which is what we are really interested in. In order to set the SCA window, we throw a switch on the TAC/SCA unit, which causes the SCA to win-

now the output of the TAC. In this mode of operation, if the output amplitude of the TAC falls within the voltage window set by the SCA, the TAC operates normally and outputs a voltage proportional to the time difference between the START and STOP pulses. However, if the output of the TAC falls outside of the SCA window, the TAC output is inhibited and there is no TAC output. Thus, if the SCA window is not properly set, no peak appears in the MCA histogram. We thus set the SCA window by simply monitoring the MCA histogram and adjusting the SCA controls until only the coincidence peak is seen and the uncorrelated background is eliminated.

## APPENDIX C: PARTS LIST AND COST OF EXPERIMENT

Here, we list the major components for this experiment. A detailed list of all the components can be found on our website.<sup>27</sup>

*Pump Laser:* Edmund Industrial Optics, (<http://www.edmundoptics.com/>). Diode-pumped, frequency-doubled, solid-state laser (405–410 nm); model NT55-872; \$5,800.

*Downconversion Crystal:* Cleveland Crystals, (<http://www.clevelandcrystals.com/>). Beta-barium borate (BBO) crystal, 3 mm long, for converting a cw 405-nm input to an 810-nm output, 3° cone angle on signal and idler, XH0503 housing with a 5-mm aperture, Humidity-barrier antireflective coatings on the crystal faces, nitrogen purge connections, and no windows; \$2,160.

*Single-Photon Counting Modules:* Pacer Components, (<http://www.pacer.co.uk/>). Single-photon counting module (Perkin Elmer model SPCM-AQR-13-FC), dark count less than 250 cps, FC fiber connector; quantity 3; \$4,300/each.

*Counting Electronics:* ORTEC, (<http://www.ortec-online.com/>). TAC/SCA model 567; nuclear instruments modular (NIM) plug-in module; quantity 3; \$1,656/each. These modules plug into a NIM crate with associated power supply, which we already had available to us. If a NIM crate is needed, the ORTEC model 4001A/4002D @ \$2,500 should be suitable. MCA model TRUMP-PCI-2K (diagnostic for setting up SCA window); PCI plug-in card with software; \$2,370.

*Counter:* National Instruments, (<http://www.ni.com/>). 8-channel counter/timer model PCI-6602; plug-in card. (Note that the optional BNC-2121 connector block and SH68-68-D1 shielded cable greatly simplify connecting to the counter). Total cost with options, \$1,000.

*Alignment Laser and Power Supply:* Thorlabs, (<http://www.thorlabs.com/>). 785-nm laser coupled to a single-mode fiber with FC connector; model LPS-4224-785-FC; \$400. ILX Lightwave, (<http://www.ilxlightwave.com/>). Current source model LDX-3412; \$930.

The total cost of the experiment is ~\$40 000. This cost includes all of the equipment necessary to carry out the experiments, with the exception of a computer, LABVIEW software, and the 3×5 foot optical table. The experiment does not require a full optical table—an optical breadboard would be sufficient, and it should be possible to fit everything on a 3×4 ft breadboard. Below, we discuss a few possibilities for reducing the cost of the experiment.

Approximately \$2,500 of the cost is for standard optical components: mirrors, kinematic mounts, posts, etc. A laboratory with a stock of such components could save much of

this cost. The fiber-coupled alignment laser and power supply are nothing special—any available laser coupled into a fiber would suffice.

Another opportunity for reducing cost is in the counting electronics. Many laboratories have some of the necessary electronics as part of existing nuclear physics experiments. Thus, it may be possible to save on the TAC/SCA cost and the cost of a NIM crate. It also is possible to build coincidence counting electronics from integrated circuits,<sup>9</sup> eliminating nearly \$7,400 in cost.

After our apparatus was assembled, Perkin Elmer introduced the SPCM-AQ4C, which consists of four fiber-coupled photon-counting modules in one unit. These modules have a larger dark count rate (500 cps), but that should have little or no affect on the experiments described here. The cost of this unit is \$9,000, which is significantly cheaper than purchasing three separate counters. If we were building a new system, we would use this unit.

We do not recommend replacing the avalanche photodiode-based photon-counting modules with photomultiplier tubes (PMTs). Quantum efficiencies of most PMTs above 800 nm are about 100 times smaller than avalanche photodiodes, meaning that the count rates would be 100 times lower. PMTs with GaAs photocathodes have efficiencies that are only 5 or 6 times lower than avalanche photodiodes, which is not too bad. However, PMT-based systems further require the use of cooled housings, high-voltage (HV) power supplies, discriminators, and possibly high speed amplifiers; this increases the cost and complexity of PMT-based systems. Even PMT-based photon-counting modules (which incorporate the housing, HV supply, and discriminator) operate significantly better with external temperature control circuitry, which makes their cost higher than the avalanche diode systems.

If a high-compliance voltage laser diode current source is already available, stand-alone 30 mW blue laser diodes are available directly from Nichia, ([www.nichia.com](http://www.nichia.com)), for \$2,000 each. It would be advisable to have a temperature-controlled mount for this diode. If a laboratory already has an Ar-ion laser, it could be used. The bluest line with significant power (10 s of mW) is typically at 458 nm, which places the downconversion at 916 nm. There is a slight reduction in quantum efficiency of the avalanche diodes at this wavelength, but we envision no significant obstacles to operating at this wavelength.

<sup>9</sup>Electronic mail: [beckmk@whitman.edu](mailto:beckmk@whitman.edu)

<sup>1</sup>R. Q. Stanley, "Question #45: What (if anything) does the photoelectric effect teach us?," *Am. J. Phys.* **64**, 839 (1996).

<sup>2</sup>P. W. Milonni, "Answer to Question #45: What (if anything) does the photoelectric effect teach us?," *Am. J. Phys.* **65**, 11–12 (1997).

<sup>3</sup>W. E. Lamb, Jr. and M. O. Scully, "The photoelectric effect without photons," in *Polarization, Matière et Rayonnement* (Presses University de France, Paris, 1969).

<sup>4</sup>L. Mandel, "The case for and against semiclassical radiation theory," in *Progress in Optics*, edited by E. Wolf (North-Holland, Amsterdam, 1976), Vol. XIII, pp. 27–68.

<sup>5</sup>D. C. Burnham and D. L. Weinberg, "Observation of simultaneity in para-

metric production of optical photon pairs," *Phys. Rev. Lett.* **25**, 84–87 (1970).

<sup>6</sup>J. F. Clauser, "Experimental distinction between the quantum and classical field-theoretic predictions for the photoelectric effect," *Phys. Rev. D* **9**, 853–860 (1974).

<sup>7</sup>H. J. Kimble, M. Dagenais, and L. Mandel, "Photon antibunching in resonance fluorescence," *Phys. Rev. Lett.* **39**, 691–695 (1977).

<sup>8</sup>A. C. Funk and M. Beck, "Sub-Poissonian photocurrent statistics: Theory and undergraduate experiment," *Am. J. Phys.* **65**, 492–500 (1997).

<sup>9</sup>D. Dehlinger and M. W. Mitchell, "Entangled photon apparatus for the undergraduate laboratory," *Am. J. Phys.* **70**, 898–902 (2002).

<sup>10</sup>D. Dehlinger and M. W. Mitchell, "Entangled photons, nonlocality, and Bell inequalities in the undergraduate laboratory," *Am. J. Phys.* **70**, 903–910 (2002).

<sup>11</sup>P. Grangier, G. Roger, and A. Aspect, "Experimental evidence for a photon anticorrelation effect on a beam splitter: A new light on single-photon interferences," *Europhys. Lett.* **1**, 173–179 (1986).

<sup>12</sup>G. Greenstein and A. G. Zajonc, *The Quantum Challenge, Modern Research on the Foundations of Quantum Theory* (Jones and Bartlett, Sudbury, MA, 1997).

<sup>13</sup>R. Hanbury Brown and R. Q. Twiss, "Correlation between photons in two coherent beams of light," *Nature (London)* **177**, 27–29 (1956).

<sup>14</sup>An excellent compilation of reprints, including many of the articles referenced here, is L. Mandel and E. Wolf, *Selected Papers on Coherence and Fluctuations of Light (1850–1966)* (SPIE, Bellingham, WA, 1990).

<sup>15</sup>R. Hanbury Brown and R. Q. Twiss, "A test of a new type of stellar interferometer on Sirius," *Nature (London)* **178**, 1046–1048 (1956).

<sup>16</sup>E. Brannen and H. I. S. Ferguson, "The question of correlation between photons in coherent light rays," *Nature (London)* **178**, 481–482 (1956).

<sup>17</sup>E. M. Purcell, "The question of correlation between photons in coherent light rays," *Nature (London)* **178**, 1449–1450 (1956).

<sup>18</sup>R. Hanbury Brown and R. Q. Twiss, "Interferometry of the intensity fluctuations in light I. Basic theory: the correlation between photons in coherent beams of radiation," *Proc. R. Soc. London, Ser. A* **242**, 300–324 (1957).

<sup>19</sup>R. Q. Twiss, A. G. Little, and R. Hanbury Brown, "Correlation between photons in coherent beams of light, detected by a coincidence counting technique," *Nature (London)* **180**, 324–326 (1957).

<sup>20</sup>R. Loudon, *The Quantum Theory of Light*, 3rd ed. (Clarendon, Oxford, 2000).

<sup>21</sup>A way to motivate the validity of this inequality is to note that the variance of the intensity must be a positive number. Since the variance can be written as  $\Delta I^2 = \langle I^2 \rangle - \langle I \rangle^2 \geq 0$ , it must be true that  $\langle I^2 \rangle \geq \langle I \rangle^2$ .

<sup>22</sup>F. T. Arecchi, E. Gatti, and A. Sona, "Time distribution of photons from coherent and Gaussian sources," *Phys. Lett.* **20**, 27–29 (1966).

<sup>23</sup>L. Mandel and E. Wolf, *Optical Coherence and Quantum Optics* (Cambridge U.P., Cambridge, 1995).

<sup>24</sup>P. L. Kelly and W. H. Kleiner, "Theory of electromagnetic field measurement and photoelectron counting," *Phys. Rev.* **136**, A316–A334 (1964).

<sup>25</sup>R. J. Glauber, "Optical coherence and photon statistics," in *Quantum Optics and Electronics*, edited by C. DeWitt-Moretz, A. Blandin, and C. Cohen-Tannoudji (Gordon and Breach, New York, 1965), pp. 63–185.

<sup>26</sup>Z. Y. Ou, C. K. Hong, and L. Mandel, "Relation between input and output states for a beamsplitter," *Opt. Commun.* **63**, 118–122 (1987).

<sup>27</sup><http://www.whitman.edu/~beckmk/QM/>

<sup>28</sup>C. K. Hong, Z. Y. Ou, and L. Mandel, "Measurement of subpicosecond time intervals between two photons by interference," *Phys. Rev. Lett.* **59**, 2044–2046 (1987).

<sup>29</sup>C. H. Holbrow, E. Galvez, and M. E. Parks, "Photon quantum mechanics and beamsplitters," *Am. J. Phys.* **70**, 260–265 (2002).

<sup>30</sup>E. J. Galvez *et al.*, personal communication, 2004.

<sup>31</sup>S. Friberg, C. K. Hong, and L. Mandel, "Measurement of time delays in the parametric production of photon pairs," *Phys. Rev. Lett.* **54**, 2011–2013 (1985).